Supplementary Material for Singular Foliations for Knit Graph Design

1 KNITTING PRIMER

We first provide a brief introduction to some basic knitting terms. The interested reader is directed to [3] and [4] for useful figures and a more detailed treatment of these topics. Weft knitting involves forming a fabric from rows of yarn loops interwoven together to form a grid of stitches. Rows of these basic stitches are known as *courses* while columns are known as *wales*. A regular grid of such stitches induces a planar geometry. To introduce curvature, *stitch irregularities* in the form of *short rows* and *increases* and *decreases* are introduced. Short rows are used to introduce additional course rows while increases/decreases change the number of wale columns. By a geometrically-informed placement of these irregularities, one can reproduce a target shape.

Using the framework established by [4], we aim to construct a *knit graph* to represent the stitch pattern. Regular stitches in the knit graph are represented by nodes that have four directed edges. Two are incoming/outgoing course edges and describe the direction in which yarn is laid down by the knitting machine. The other two are incoming/outgoing wale edges and describe the direction in which course rows are being produced. Short row ends are formed by nodes which lack either an incoming or outgoing course edge. Increase/decreases are formed by nodes have more than one outgoing/incoming wale edge. Finally, the most challenging knit graph constraint introduced by [4] is the *helix-free* condition, i.e., any course row may not intersect the same wale column twice. Such a structure would require knitting a course row of loops onto a course row that has not yet been knit. Knittability in this work is defined as the ability to satisfy all of [4] graph constraints.

2 SPINNING FORM LEVEL SETS ON SINGULAR TRIANGLES

Here, we derive explicit analytic expressions for the integral curves and flow structure in singular triangles. As noted in the text, this is done via analysis of the level sets of φ, the texture interpolant of [2]. First, we recall some notation and definitions.

Consider a singular triangle with vertices i, j, k oriented counterclockwise, and oriented spinning form values along the edges given by $\sigma_{ij}, \sigma_{jk}, \sigma_{ki}$. Let α_i be the local value of the spinning form integrated along an arbitrary spanning tree of mesh edges, and define:

$$\alpha_j := \alpha_i + \sigma_{ij} \qquad \& \qquad \alpha_k := \alpha_j + \sigma_{jk}, \tag{1}$$

to be the representative values at vertices j and k. Recall that when one considers these values modulo 2π (or P, user-defined period), the spinning form results in a well-defined function to $\mathbb{S}^1$, regardless of what spanning tree is used. The singular triangle has stripe index n, and the stripe pattern overall has period P, so that:

$$\sigma_{ij} + \sigma_{jk} + \sigma_{ki} = nP. \tag{2}$$

Barycentric coordinates on the triangle are denoted b_i, b_j, b_k. Our texture interpolant φ is defined piecewise over barycentric regions of the triangle:

$$\varphi = b_i\alpha_i + b_j\left(\alpha_j - \frac{nP}{3}\right) + b_k\left(\alpha_k - \frac{2nP}{3}\right) + \mathrm{lArg}_n(b_i, b_j, b_k), \tag{3}$$

$$\mathrm{lArg}_n(b_i, b_j, b_k) = \begin{cases} \frac{nP}{6}\left(1 + \frac{b_j - b_i}{1-3b_k}\right), & b_k \le b_i \;\&\; b_k \le b_j \text{ (region 1)} \\ \frac{nP}{6}\left(3 + \frac{b_k - b_j}{1-3b_i}\right), & b_i \le b_j \;\&\; b_i \le b_k \text{ (region 2)} \\ \frac{nP}{6}\left(5 + \frac{b_i - b_k}{1-3b_j}\right), & b_j \le b_k \;\&\; b_j \le b_i \text{ (region 3)} \end{cases}$$

Intuitively, this function provides a discontinuous jump of nP at the boundary between regions 1 & 3, a necessity due to the non-integrability of σ.

2.1 Region Boundary Behavior

At this point, let us note the behavior of φ along the boundary of the triangle and the boundaries between barycentric regions. First, along triangle edges, lArg_n is linear as $b_k = 0$ along ij, $b_i = 0$ along jk, and $b_j = 0$ along ki. Thus, φ linearly interpolates:

$$\alpha_i \to \alpha_j \text{ along } ij \qquad \alpha_j \to \alpha_k \text{ along } jk \qquad \alpha_k \to \alpha_i + nP \text{ along } ki \tag{4}$$

The lArg_n function is constant along rays to the barycenter, as noted in [2] (see Fig. 13 and "Zeros" section), so we get that φ is also linear along barycentric region boundaries. Let $\alpha_{mid} := (\alpha_i + \alpha_j - nP/3 + \alpha_k - 2nP/3)/3$ denote the value taken by the linear part of φ at the triangle barycenter, denoted mid. The linear interpolatory behavior at the barycentric region boundaries is then:

$$\alpha_i \to \alpha_{mid} \quad \text{along} \quad i \to mid \ \ (\text{from R1}) \tag{5}$$

$$\alpha_j \to \alpha_{mid} + \frac{nP}{3} \quad \text{along} \quad j \to mid \tag{6}$$

$$\alpha_k \to \alpha_{mid} + \frac{2nP}{3} \quad \text{along} \quad k \to mid \tag{7}$$

$$\alpha_i + nP \to \alpha_{mid} + nP \quad \text{along} \quad i \to mid \ \ (\text{from R3}). \tag{8}$$

Note that the jump discontinuity of nP along the boundary between R1 and R3 result in two behaviors along the segment $i \to mid$, depending on which region you approach from.

As lArg_n takes values ranging from 0 to nP along rays to the barycenter, one can also see that φ is undefined at mid, and takes values between α_{mid} and $\alpha_{mid} + nP$, depending on which direction you approach from. This results in the first small lemma characterizing the level set/foliation structure in singular triangles:

Lemma 1. *For any singular triangle, leaves (level sets/integral curves) meet at a source or sink singularity at the barycenter, when $nP > 0$ and $nP < 0$, respectively.*

Moreover, with the analysis above, we have determined the level set behavior on the boundaries of each barycentric region, and just need to determine the structure of level sets in the region interiors.

2.2 Region Interior Analysis

In the arguments below, we present just the relevant arguments in region 1, R1 ($b_k \le b_i$ & $b_k \le b_j$), and for $nP > 0$, for brevity and clarity. The arguments for other regions and for $nP < 0$ are entirely analogous, and follow via permutation of some of the symbols and some sign switches. All of the lemmas rely on putting the quadratic interpolant into a standardized form, so we describe this below for R1. Singular triangle level sets are exactly those that satisfy $\varphi = C$, for some constant C:

$$C = \alpha_i b_i + \left(\alpha_j - \frac{nP}{3}\right) b_j + \left(\alpha_k - \frac{2nP}{3}\right)(1 - b_i - b_j) + \frac{nP}{6}\left(1 + \frac{b_j - b_i}{3b_i + 3b_j - 2}\right). \tag{9}$$

Above, we have expressed things just in terms of b_i, b_j, using the fact that $b_k = 1 - b_i - b_j$. After clearing the denominator on the last term and shifting things all to one side, we have a quadratic expression in b_i, b_j. We can complete the square to put it into a more interpretable form:

$$\mathbf{x}^T \mathbb{A} \mathbf{x} + \mathbf{x}^T \mathbf{b} + c_* = (\mathbf{x} - \mathbf{h})^T \mathbb{A} (\mathbf{x} - \mathbf{h}) + k = 0, \tag{10}$$

where $\mathbf{x} = (b_i, b_j)$ and $\mathbb{A}, \mathbf{b}, \mathbf{h}, k, c^*$ are a constant symmetric 2×2 matrix, two constant 2×1 matrices, and two scalar constants, respectively. The matrix $\mathbb{A} = \left[\begin{smallmatrix} a & b \\ b & c \end{smallmatrix}\right]$ of quadratic term coefficients is:

$$\begin{aligned} a &= 2nP + 3\alpha_i - 3\alpha_k \\ b &= \frac{3nP + 3\alpha_i + 3\alpha_j - 6\alpha_k}{2} \\ c &= nP + 3\alpha_j - 3\alpha_k. \end{aligned} \tag{11}$$

The linear term coefficients and constant term is:

$$\mathbf{b} = \begin{bmatrix} -3nP - 2\alpha_i + 5\alpha_k - 3C \\ -2nP - 2\alpha_j + 5\alpha_k - 3C \end{bmatrix} \qquad \& \qquad c^* = nP - 2\alpha_k + 2C \tag{12}$$

There are simple formulae for both $\mathbf{h}$ and k in terms of $\mathbb{A}, \mathbf{b}, c^*$:

$$\mathbf{h} = -\frac{1}{2}\mathbb{A}^{-1}\mathbf{b} \qquad \& \qquad k = c_* - \frac{1}{4}\mathbf{b}^T\mathbb{A}^{-1}\mathbf{b}, \tag{13}$$

which we will evaluate later in our exposition. We call $\mathbf{h}$ and k the *center* and *shift* of the hyperbolic level set, respectively, and are analogous to the origin and level set constant D for the standard hyperbola: $x^2 - y^2 = D$. Thus, they give geometric information about the location and topological nature of the level set, respectively. In particular for $k = 0$, we obtain a union of lines, and this will result in a saddle singularity for the foliation at $\mathbf{h}$. For $k > 0$ or $k < 0$, we obtain regular hyperbolic level sets "opening" in different directions.

The first lemma that we argue shows that the level sets are generally hyperbolae in barycentric coordinates, and that the level sets on the triangle as a whole are unions of these hyperbolae meeting each other at the barycentric region boundaries.

Lemma 2. *Within each singular triangle, foliation leaves are unions of hyperbolae defined in each barycentric region, in terms of barycentric coordinates.*

Proof. We argue this fact in region 1 ($b_k \leq b_i$ & $b_k \leq b_j$), and note that the arguments in other regions follow by symmetry. The type of level sets (hyperbolae, ellipses, parabolas) are determined by the eigenvalues of $\mathbb{A}$, the quadratic form. In particular, noting that $b = (a + c)/2$, we find that the eigenvalues are given by:

$$\lambda_{\mathbb{A}} = \frac{(a + c) \pm \sqrt{(a + c)^2 - 4(ac - b^2)}}{2} = \frac{(a + c) \pm \sqrt{2(a^2 + c^2)}}{2}.$$

With nonnegative discriminant, it is clear that the eigenvalues are real, and now we simply need to check that their signs differ to finish our argument. For this, we simply compare the magnitude of the two numerator terms:

$$|a + c| \leq \sqrt{2(a^2 + c^2)} \Leftrightarrow (a + c)^2 \leq 2(a^2 + c^2) \Leftrightarrow 2ac \leq a^2 + c^2 \Leftrightarrow 0 \leq (a - c)^2.$$

Thus, our quadratic form generally has opposite sign eigenvalues, and the level sets are hyperbolae. □

Now, let us note that the center and shift, $\mathbf{h}$ and k, of each level set $\varphi = C$ depend on C and that they are linear functions of C via Eqs. (13) and (12). Hence our level sets are not simply analogous to the level sets of a standard fixed quadratic hyperbola: $x^2 - y^2 = D$, as the constants in the defining equation are changing as C changes. All the same, as they are level sets of a function, φ, so they may not cross each other and their topological relation to each other should remain the same. Thus, the center of the level set with $k = 0$ presents the *only* opportunity for any singularity of the foliation structure in the barycentric region interiors given by the level sets. $k = 0$ occurs for the value:

$$\tilde{C} := \frac{\alpha_i^2 - \alpha_j^2 + nP\alpha_j - \alpha_j\alpha_k + \alpha_i\alpha_k}{nP - 3\alpha_j + 3\alpha_i}, \tag{14}$$

.

and results in a center:

$$\tilde{\mathbf{h}} := \begin{bmatrix} \tilde{b}_i \\ \tilde{b}_j \end{bmatrix} = \frac{1}{(3\alpha_i - 3\alpha'_j)^2} \begin{bmatrix} 3(\alpha_i - \alpha'_j)^2 + nP(\alpha'_k - \alpha'_j) \\ 3(\alpha_i - \alpha'_j)^2 + nP(\alpha_i - \alpha'_k) \end{bmatrix}, \tag{15}$$

where $\alpha'_j = \alpha_j - \frac{nP}{3}$ and $\alpha'_k = \alpha_k - \frac{2nP}{3}$ have been introduced to make notation more compact.

Now, we tackle our sign-based characterization of the foliation structure. In the text below, we first argue that the center of any given hyperbolic section lies outside the triangle, if we are in the + + + case.

Lemma 3. *For a singular triangle, if $\sigma_{ij}, \sigma_{jk}, \sigma_{ki} > 0$, then the center $\tilde{\mathbf{h}}$ of the hyperbolic sections in each barycentric region lie outside the region itself (and thus the triangle has no singularities interior to any barycentric region).*

Proof. As before, we argue in region 1 only. For the center of the zero shift level set to lie in region 1, it must satisy three inequalities simultaneously: $\tilde{b}_k \leq \tilde{b}_i, \tilde{b}_k \leq \tilde{b}_j, \tilde{b}_k \geq 0$. Above, $\tilde{b}_k = 1 - \tilde{b}_i - \tilde{b}_j$ denotes the third barycentric coordinate of $\tilde{\mathbf{h}}$ and after plugging in the expressions for $\tilde{b}_i, \tilde{b}_j$ we obtain:

$$\tilde{b}_k = \frac{1}{3} - \frac{nP}{9(\alpha_i - \alpha'_j)} = \frac{1}{3}\left(1 + \frac{nP}{3\sigma_{ij} - nP}\right) \tag{16}$$

We show now that assuming the first two of these inequalities implies that the last does not hold, proving our lemma. Recalling that $\alpha_j = \alpha_i + \sigma_{ij}$, $\alpha_k = \alpha_j + \sigma_{jk}$, and $\sigma_{ij} + \sigma_{jk} + \sigma_{ki} = nP$, some algebra reveals that:

$$\frac{9(\alpha_i - \alpha'_j)^2}{nP}(\tilde{b}_i - \tilde{b}_k) = \sigma_{jk} - \sigma_{ij} \qquad \& \qquad \frac{9(\alpha_i - \alpha'_j)^2}{nP}(\tilde{b}_j - \tilde{b}_k) = \sigma_{ki} - \sigma_{ij} \tag{17}$$

If the first two assumptions hold, then the two expressions above are positive and $\sigma_{jk} > \sigma_{ij}$ and $\sigma_{ki} > \sigma_{ij}$. As these three all sum to nP, this implies that $\sigma_{ij} < (nP)/3$, which implies that $\tilde{b}_k < 0$ by Eqn. (16). □

With this, we can characterize the level set structure in each barycentric region as consisting of hyperbolic segments that radiate out from the barycenter. This follows from the fact that the boundary takes on values increasing from α_i to $\alpha_i + nP$ monotonically along the boundary.

The characterization of the cases + + − and + − − are obtained via the following lemma.

Lemma 4. *For $nP > 0$, and in the + + − or + − − cases, the barycentric region bounded by the edge with least σ (note: negative) contains a hyperbola center, and thus a saddle singularity. Hyperbola centers do not appear in other barycentric regions. Similarly, for $nP < 0$, and in the − − + or − + + cases, the barycentric region bounded by the edge with greatest σ (note: positive) contains a hyperbola center, and thus a saddle singularity. Hyperbola centers do not appear in other barycentric regions.*

Proof. As before, we argue for just the $nP > 0$ case, and consider σ_{ij} to be the least value. Looking at R1, we still have the above expressions Eqs. (16), (17). We aim to show that all three inequalities hold: $\tilde{b}_k \leq \tilde{b}_i, \tilde{b}_k \leq \tilde{b}_j, \tilde{b}_k \geq 0$. The first two hold via Eq. (17) as $\sigma_{ij} < \sigma_{jk}$ and $\sigma_{ij} < \sigma_{ki}$, and the last one holds via Eq. (16). In particular, with $\sigma_{ij} < 0$, we have that $-1 < nP/(3\sigma_{ij} - nP) < 0$ and thus $\tilde{b}_k > 0$. Analogous arguments show that the hyperbolic centers in R2 and R3 can't be in those regions as $\sigma_{ij} < \sigma_{jk}$ and $\sigma_{ij} < \sigma_{ki}$, respectively. □

2.3 Algebraic expressions for separatrix level sets

Let us first characterize the separatrices in a barycentric region, when it contains the hyperbola center $\tilde{\mathbf{h}}$. Note that both axes of separatrices are linear on the triangle, as the map from barycentric coordinates onto the triangle is affine. We begin with a lemma that shows that one such separatrix axis is parallel to the triangle edge that bounds the region.

Lemma 5. *Two separatrices (one separatrix axis) are parallel to the triangle edge that is part of the barycentric region containing the center of the hyperbola* $\tilde{\mathbf{h}}$.

Proof. We will argue in the case of R1, and $nP > 0$, as usual. Assume that we have the separatrix axis described parametrically in barycentric coordinates b_i, b_j as $\gamma(t) = \tilde{\mathbf{h}} + t\mathbf{v}$ where $\mathbf{v} = [v_i, v_j]^T$ denotes a "velocity" vector. As the triangle edge $\vec{e}_{ij}$ is described parametrically as $[1, 0]^T + t[-1, 1]^T$, we can prove our result by showing that $v_i = -v_j$. From Eq. (11) we have the quadratic form coefficients, and we know that $\mathbf{v}$ will satisfy $\mathbf{v}^T \mathbb{A} \mathbf{v} = 0$. Writing this out, we have:

$$\begin{bmatrix} v_i & v_j \end{bmatrix} \begin{bmatrix} a & b \\ b & c \end{bmatrix} \begin{bmatrix} v_i \\ v_j \end{bmatrix} = 0 \implies a v_i^2 + 2 b v_i v_j + c v_j^2 = 0 \implies v_i = \left(\frac{-b \pm \sqrt{b^2 - ac}}{a} \right) v_j$$

Recalling that $b = (a+c)/2$, we can see that the minus case in the quadratic formula results in our desired equality $v_i = -v_j$. □

The other separatrix axis, which we refer to as the *source separatrix* (or *sink separatrix* if $nP < 0$), must have a trajectory that exits the source singularity at the barycenter via our foliation structure characterization. At this point, we may use the separatrix level set value $\tilde{C}$ from Eq. (14) to determine the birth/death interval endpoints on the boundary of the triangle, as well as the point at which the source separatrix impacts the boundary.

In short, given the parallel nature of one separatrix axis, we know that it will impact the boundaries of the barycentric region coming into the barycenter, and will continue into neighboring regions. As the behavior of φ is linear along the triangle boundaries, it is simple to linearly interpolate to find where the continued level sets will intersect the boundary. For the source separatrix axis, we may simply do the same, but along the edge which forms the barycentric region boundary.

3 PROPOSITION 1 PROOF

In this section, we make the necessary definitions and arguments to prove Prop. 1, which shows us that we can achieve non-helicing of cell level sets by using non-helicing level set constraints.

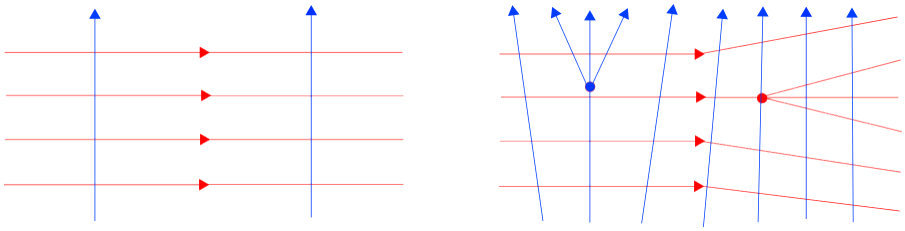

Fig. 1. Transversals and transverse foliations examples. Left: blue curves are *transversals* to the red foliation. Right: blue and red foliations are *transverse* to each other; dots denote singularities and effective interpolant represented schematically nearby.

First, we define what it means for two foliations to be *transverse*. In particular, we extend the definition of a *transversal* curve to a foliation made in §1.4.1 of [1]. A curve $\gamma : [0, 1] \to M$ is a transversal if in the neighborhood of any point $\gamma(t)$ for $t \in (0, 1)$ there is a rectifying diffeomorphism carrying γ onto $\{0\} \times \mathbb{R}$. In essence, γ is never tangent to the foliation. A foliation σ_c is *transverse* to another σ_w if each of its nonsingular (non-fixed-point) trajectories is a transversal of σ_c (away from singularities of σ_w where there are no rectifying diffeomorphisms). Fig. 1 shows local views of transversals and transverse foliations.

A leaf (candidate course row) of σ_c forms a *helix* with respect to a leaf (candidate wale column) of σ_w if it intersects the leaf in two distinct places (compare to Property 2 of §3.2 of [4]). We note here that we allow wale leaves to "continue" through wale singularities as this captures the analogous notion of candidate wale column in the machine-knitting setting (see an example in the bold blue wale leaf in Fig. 3).

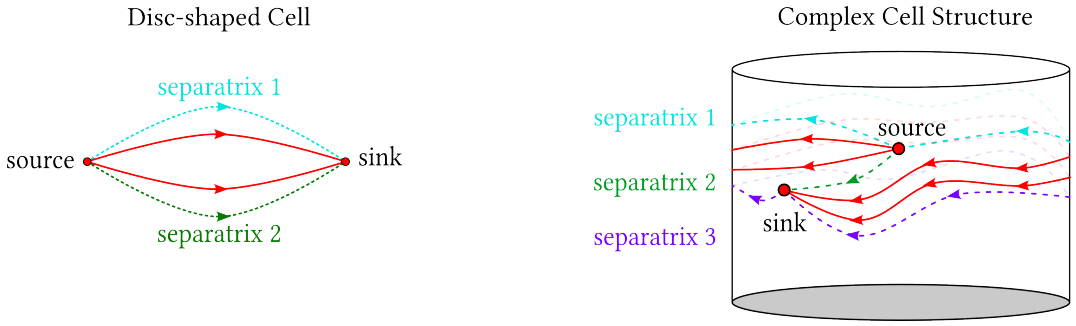

Fig. 2. "Boundaries" of a disc-shaped cell. Left: a simple cell in a red foliation; one boundary is formed by separatrix 1 (cyan) and another is formed by separatrix 2 (green). Right: A more complicated cell in a red foliation on a cylinder; one boundary is formed by the sequence {separatrix 1 (cyan), source, separatrix 2 (green) } and another is formed by the sequence {separatrix 2 (green), sink, separatrix 3 (purple) }.

Now, we note that the boundary of a disc-shaped (homeomorphic to) cell R in the orbit complex of σ_c is made up of sequences of separatrices and fixed points joining a source and sink singularity that form the endpoints of the parallel flow on the cell. The source and sink singularities split ∂R into two ordered sequences, that we refer to as the two "boundaries" of R in the proposition. They are the *schemes* of the two semi-cells that make up R (see §6.5.1 & 6.5.3 in [1]). We illustrate some examples in Fig. 2.

Proposition 1. *Consider two transverse course and wale foliations specified by σ_c, σ_w, and our effective interpolant. In any disc-shaped cell R in the orbit complex of σ_c, if either boundary of R is helix-free with respect to σ_w, then all integral curves of R are helix-free.*

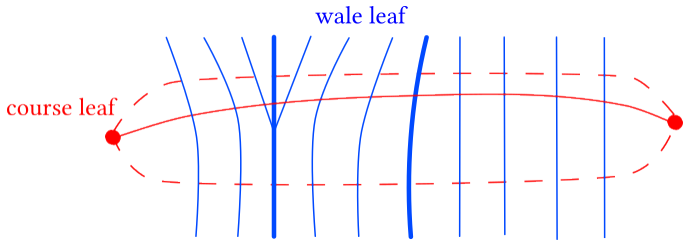

Fig. 3. Proof sketch. σ_c foliation in red, and σ_w foliation in blue. Course leaf l_c represented by the solid red line, and wale leaf l_w represented by the bolded blue line. If l_c crosses l_w twice then it must cross both boundaries of R twice.

Proof. Our argument is illustrated in Fig. 3. First, note that it illustrates the structure of the foliations σ_c and its transverse σ_w in cell R. Now, let us make an argument by contradiction: suppose an interior leaf l_c of R helices with respect to some leaf l_w of σ_w. Due to the two foliations being transverse, this means that l_w must pass through R at least twice, crossing all of the course leaves in R. Thus, it intersects both boundaries of R twice and we get that both boundaries helix with respect to l_w, a contradiction. □

4 CYLINDER DECOMPOSITION

In this section, we describe the process by which we decompose more topologically complex M ($n > 2$ boundaries and/or genus $g > 0$) into cylindrical components. This decomposition is based on ideas from Morse theory, and a view of the knitting time function h as a Morse function. In particular, the sublevel sets $h_{\leq E} := \{p \in M \mid h(p) < E\}$ for some constant $E \in \mathbb{R}$ change topology as E takes on *critical values*. A *critical point* is a point $p \in M$ such that $dh(p) = 0$, and the values of h at such points are the critical values. Discretely, these critical points arise as *saddle*

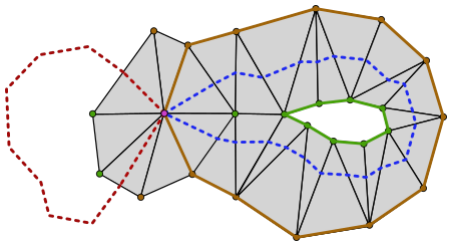

Fig. 4. Time function isolines (red and blue) near a saddle point (pink) with bounding edge loops (green and orange).

points of the time function, h. These are vertices v of the mesh where the value of $h(w) - h(v)$ on neighboring vertices w changes sign more than twice as you circulate about v (the number is always even). An example is illustrated in Fig. 4. With probability one, saddle points will have four sign changes, and the level set of $h(v)$ will have four line segments emanating from v. We must find two edge loops that pass through v and roughly trace the level sets of h. Note in general, the time function isoline does not lie exactly on the edges of the mesh.

Thus, our procedure (schematic in Fig. 4) for generating these edge loops begins by following one adjacent segment and tracking the isoline. As we go, we collect all of the triangles that the isoline intersects. Then, we extract the boundary edges from this triangle strip, resulting in two loops that bound the time function isoline from above and below. Both roughly follow the critical level set, so we arbitrarily choose the one that bounds above. The process is repeated for the other two adjacent line segments.

.

Algorithm 1: Cylindrical Decomposition

Input: Saddle point, v
Output: Two Saddle Edge loops, $\{e_1^1, \ldots, e_n^1\}, \{e_1^2, \ldots, e_m^2\}$
Function `CylindricalDecomposition(`v`)`

```
t_v ← TimeFunction(v);
UniqueTriangleStrips = [];
[h_1, h_2, h_3, h_4] ← CriticalHalfedges(v, t_v);
for h ∈ [h_1, h_2, h_3, h_4] do
    currHe ← h.twin() ;    // First halfedge should *not* be on the same triangle as v
    nextHe ← NextHalfedgeOnIsoline(t_v, currHe);
    T_strip = [h.face(), currHe.face()];
    // Traverse isoline triangle strip.
    while currHe.face() != nextHe.face() do
        currHe ← nextHe;
        nextHe ← NextHalfedgeOnIsoline(t_v, currHe);
        T_strip.append(currHe().face());
    // Extract unique triangle strips.
    if T_strip ∉ UniqueTriangleStrips then
        UniqueTriangleStrips.append(T_strip);
        boundingLoops ← uniqueEdges(T_strip);
        saddleLoop ← chooseUpperLoop(boundingLoops);
        SaddleEdgeLoops.append(saddleLoop)
return SaddleEdgeLoops
```

Algorithm 2: Saddle Point Isoline Tracing

Input: Time Function Value, t_v; Halfedge, he
Result: Halfedge
Function `NextHalfedgeOnIsoline(`t_v, he`)`

```
next ← he.next();
prev ← he.prev();
// Store the min. and max. values of the time function on the endpoints
(nextMin, nextMax) ← getMinMax(next);
(prevMin, prevMax) ← getMinMax(prev);
// Return the *twin* of the halfedge that contains the isoline value.
if t_v ∈ (nextMin, nextMax) then
    return next.twin();
else if t_v ∈ (prevMin, prevMax) then
    return prev.twin();
else
    return he;
```

Algorithm 3: Finding Critical Saddle Point Halfedges

Input: Vertex, v; Time Function Value, t_v;
Result: Halfedges, $[h_1, h_2, h_3, h_4]$
Function `CriticalHalfedges`(v, t_v)
  `// Check the halfedges opposite the vertex` v
  for $he \in$ ***outgoingHalfedges***(v) **do**
    oppHe $\leftarrow$ $he.next()$;
    $(t_{min}, t_{max}) \leftarrow getMinMax(oppHe)$;
    if $t_v \in (t_{min}, t_{max})$ **then**
      critialHalfedges.**append**$(oppHe)$;
  return *criticalHalfedges*

5 EFFECTIVE INTERPOLANT TRACING

Here, we describe our procedure for tracing our *effective interpolant* on singular triangles. Our interpolant robustly traces level sets into such triangles and avoids the issue of a single wale column intersecting the same course row multiple times as can occur when using Knoppel's interpolant [2] as seen in Fig 5 (left).

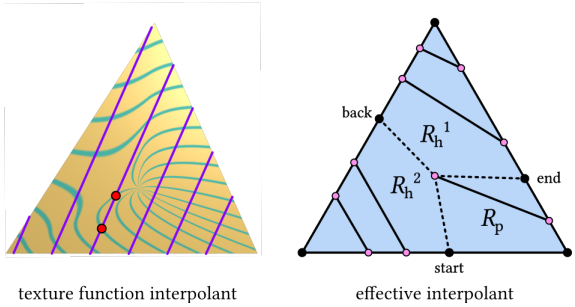

Fig. 5. A schematic diagram of knit graph connections using the effective interpolant. R_{h^1} and R_{h^2} represent the hyperbolic sectors of the ground-truth texture function interpolant, while R_p represents the parabolic sector. The integral curves intersect the triangle at boundary (pink) and are connected "outside-in" counter-clockwise on each of the hyperbolic sectors and connected to the barycenter in the parabolic sector.

Based on the intersection of separatrices with the triangle boundary, we split singular triangles into three sectors, R_{h^1}, R_{h^2} and R_p which represent the two hyperbolic sectors and the parabolic sector of our effective interpolant, respectively. These intersections with the triangle boundary are connected with the barycenter to form the new separatrices of our effective interpolant.

Within R_p our interpolant connects every integral curve that crosses the triangle boundary within the birth/death interval to the barycenter. On the other hand, integral curves that cross the boundary into the hyperbolic regions R_{h^1} and R_{h^2} must exit/enter out of the same region. As such, we pair the level sets that intersect the triangle in a hyperbolic region "outside-in" counter-clockwise. Since integral curves that enter a hyperbolic sector must necessarily exit the same sector, this matching will always be valid and will guarantee the absence of multiple intersections with a single wale column.

•

REFERENCES

[1] S. Kh. Aranson, G.R. Belitsky, and E.V. Zhuzhoma. 1996. *Introduction to the Qualitative Theory of Dynamical Systems on Surfaces*. Translations of Mathematical Monographs, Vol. 153. American Mathematical Society.

[2] Felix Knöppel, Keenan Crane, Ulrich Pinkall, and Peter Schröder. 2015. Stripe patterns on surfaces. *ACM Transactions on Graphics* 34, 4 (July 2015), 39:1–39:11.

[3] Rahul Mitra, Liane Makatura, Emily Whiting, and Edward Chien. 2023. Helix-Free Stripes for Knit Graph Design. In *ACM SIGGRAPH 2023 Conference Proceedings*. 1–9.

[4] Vidya Narayanan, Lea Albaugh, Jessica Hodgins, Stelian Coros, and James Mccann. 2018. Automatic Machine Knitting of 3D Meshes. *ACM Transactions on Graphics* 37, 3 (Aug. 2018), 35:1–35:15.